

RUGGED METROPOLIS SAMPLING WITH SIMULTANEOUS UPDATING OF TWO DYNAMICAL VARIABLES

Bernd A. Berg^{a,b} and Huan-Xiang Zhou^{a,b,c}

^{a)} *Department of Physics, Florida State University, Tallahassee, FL 32306-4350*

^{b)} *School of Computational Science, Florida State University, Tallahassee, FL 32306-4120*

^{c)} *Institute of Molecular Biophysics, Florida State University, Tallahassee, FL 32306-4380*

(April 28, 2019)

The Rugged Metropolis (RM) algorithm is a biased updating scheme, which aims at directly hitting the most likely configurations in a rugged free energy landscape. Details of the one-variable (RM₁) implementation of this algorithm are presented. This is followed by an extension which includes simultaneous updating of two dynamical variables (RM₂). For the test case of Met-Enkephalin in vacuum at 300 K the RM₁ version improves conventional Metropolis simulations by a factor of two and another factor of two is gained by switching to RM₂. We also investigate a multi-hit Metropolis scheme, which spends more CPU time on variable with large autocorrelation times, and find additional performance gains.

PACS: 05.10.Ln, 87.15-v, 87.14.Ee.

Simulations of biomolecules are one of the major challenges in computational science. Rugged free energy landscapes are typical for such systems. In this context a Rugged Metropolis (RM) algorithm was introduced in Ref. [1]. It is a Metropolis scheme for simulations of the conventional Gibbs canonical ensemble of statistical physics for which the updating proposals are biased by incorporating information from previous simulations at higher temperatures. The physical intuition for the RM scheme is based on a funnel picture of protein folding, which was originally formulated by Bryngelson and Wolynes [2].

RM is distinct from generalized ensemble simulations. Generalized ensembles (for reviews and recent work see [3]) also use information from higher temperatures, but in an entirely different way. In a sense generalized ensembles build bridges in a rugged free energy landscape, while the RM scheme enhances the likelihood for a direct hit of the needle in the haystack. That “needle” may have a high statistical probability in the canonical ensemble, but nevertheless can not be found by the conventional Metropolis algorithm due to free energy barriers. RM and generalized ensemble schemes can be combined and in a tested case the improvement was multiplicative [1].

The main challenge within the RM scheme is to obtain an efficient estimate of the multi-variable probability density from available time series data. So far this was achieved only for one-variable updates and details are given in the next section. However, it is well-known that one needs multi-variable moves to avoid steric clashes [4], see [5] and references therein for more recent literature. As a modest step in this direction, in this article two-variable updates are studied within the RM scheme.

In the next section we review the RM scheme and present Monte Carlo (MC) results for the RM₁ approximation, filling in many details which inevitably had to be omitted in the letter format of Ref. [1]. All our simulations are done for the brain peptide Met-Enkephalin

in vacuum, which has been a frequently used test case since its initial numerical investigation in Ref. [6]. Integrated autocorrelation times (see, e.g., Ref. [7] for the definition) were measured to determine the algorithmic performance. On the fly we also investigate a multi-hit updating procedure, which spends more computer time on variables with large integrated autocorrelation times. In section II we extend the RM simulation to the simultaneous updating of two dynamic variables, i.e., the RM₂ approximation. Summary and conclusions follow in section III.

I. RM AND THE RM₁ APPROXIMATION

We consider biomolecule models for which the energy E is a function of a number of dynamical variables v_i , $i = 1, \dots, n$. The fluctuations in the Gibbs canonical ensemble are described by a probability density (pd) $\rho(v_1, \dots, v_n; T)$, where T is the temperature. To be definite, we use in the following the all-atom energy function [8] ECEPP/2 (Empirical Conformational Energy Program for Peptides). Our dynamical variables v_i are the dihedral angles, each chosen to be in the range $-\pi \leq v_i < \pi$, so that the volume of the configuration space is $K = (2\pi)^n$. Details of the energy functions are expected to be irrelevant for the algorithmic questions addressed here. Our test case will be the small brain peptide Met-Enkephalin, which features 24 dihedral angles as dynamical variables, see table I (the conventions follow Ref. [9], which differs from [6]). The performance of the algorithm is tested at 300 K using input from a simulation at 400 K. The value of 300 K is chosen because it is in the range of interest to biological molecules. The temperature of 400 K is high enough so that the conventional Metropolis algorithm is efficient, while it is low enough to provide useful input for the 300 K simulation. Besides the ϕ , ψ angles, we keep also the ω angles uncon-

strained, which are usually restricted to $[\pi - \pi/9, \phi + \pi/9]$. This allows us to illustrate the RM idea for a particularly simple case.

TABLE I. Acceptance rates for dihedral angle movements. They are accurate to about ± 1 in the last digit.

var	angle	residues	400 K	300 K	300 K
			Metro	Metro	RM ₁
v_1	χ^1	Tyr-1	0.107	0.070	0.272
v_2	χ^2	Tyr-1	0.182	0.128	0.343
v_3	χ^6	Tyr-1	0.497	0.377	0.680
v_4	ϕ	Tyr-1	0.392	0.340	0.547
v_5	ψ	Gly-2	0.096	0.044	0.139
v_6	ω	Gly-2	0.049	0.034	0.416
v_7	ϕ	Gly-2	0.112	0.045	0.076
v_8	ψ	Gly-3	0.106	0.038	0.064
v_9	ω	Gly-3	0.041	0.025	0.301
v_{10}	ϕ	Gly-3	0.088	0.035	0.070
v_{11}	ψ	Phe-4	0.115	0.040	0.077
v_{12}	ω	Phe-4	0.047	0.030	0.368
v_{13}	χ^1	Phe-4	0.109	0.086	0.277
v_{14}	χ^2	Phe-4	0.192	0.166	0.403
v_{15}	ϕ	Phe-4	0.082	0.042	0.139
v_{16}	ψ	Met-5	0.122	0.063	0.156
v_{17}	ω	Met-5	0.062	0.047	0.573
v_{18}	χ^1	Met-5	0.117	0.092	0.362
v_{19}	χ^2	Met-5	0.159	0.121	0.585
v_{20}	χ^3	Met-5	0.269	0.211	0.709
v_{21}	χ^4	Met-5	0.455	0.385	0.833
v_{22}	ϕ	Met-5	0.129	0.086	0.258
v_{23}	ψ	Met-5	0.378	0.267	0.469
v_{24}	ω	Met-5	0.114	0.096	0.873
E			0.168	0.119	0.375

The Metropolis importance sampling would be perfected, if we could propose new configurations $\{v'_i\}$ with their canonical pd (rejection free Monte Carlo). Obviously, this is not possible for the systems we are interested in. But conventional Metropolis simulations work well at sufficiently high temperatures T' and provide an *estimate* $\bar{\rho}(v_1, \dots, v_n; T')$ of the pd $\rho(v_1, \dots, v_n; T')$. Due to the funnel picture we expect [1] that such an *estimate* can be used to feed useful information into the simulation at a sufficiently close-by lower temperature $T < T'$. The idea of the RM scheme is to propose a transition from a configuration $\{v_i\}$ to a new configuration $\{v'_i\}$ with the pd $\bar{\rho}(v'_1, \dots, v'_n; T')$ and to accept it with the probability

$$P_a = \min \left[1, \frac{\exp(-\beta E') \bar{\rho}(v_1, \dots, v_n; T')}{\exp(-\beta E) \bar{\rho}(v'_1, \dots, v'_n; T')} \right] \quad (1)$$

where $\beta = 1/(kT)$. This equation biases the a-priori probability of each dihedral angle with an estimate of its pd from a higher temperature. Other biased updating schemes were successfully used in the statistical physics [10,11] as well as in the bio-chemical literature [12,13,5].

For a range of temperatures

$$T_1 > T_2 > \dots > T_r > \dots > T_{f-1} > T_f \quad (2)$$

the simulation at the highest temperature, T_1 , is performed with the usual Metropolis algorithm and the results are used as input for the simulation at T_2 . When $\bar{\rho}(v_1, \dots, v_n; T_{r-1})$ is a useful approximation of $\rho(v_1, \dots, v_n; T_r)$, the scheme is supposed to zoom in on the native structure which is dominant at the physically relevant final temperature T_f .

To get things started, we need to construct an estimator $\bar{\rho}(v_1, \dots, v_n; T_r)$ from the numerical data of the RM simulation at temperature T_r . Although this is neither simple nor straightforward, a variety of approaches offer themselves to define and refine the desired estimators.

In Ref. [1] the approximation

$$\bar{\rho}(v_1, \dots, v_n; T_r) = \prod_{i=1}^n \bar{\rho}_i^1(v_i; T_r) \quad (3)$$

was investigated, where $\bar{\rho}_i^1(v_i; T_r)$ are estimators of reduced one-variable pds defined by

$$\rho_i^1(v_i; T) = \int_{-\pi}^{+\pi} \prod_{j \neq i} dv_j \rho(v_1, \dots, v_n; T) . \quad (4)$$

The resulting algorithm, called RM₁, constitutes the simplest RM scheme possible.

Let us fill in the details of the RM₁ implementation [1]. To update with the RM₁ weights it is convenient to rely on the cumulative distribution functions defined by

$$F_i(v) = \int_{-\pi}^v dv' \rho_i^1(v') . \quad (5)$$

The estimate of F_{10} , the cumulative distribution function for the dihedral angle Gly-3 ϕ (v_{10}), from the vacuum simulations at 400 K is shown in Fig. 1. This is the same angle for which histograms at 400 K and 300 K are shown in Ref. [1]. For our plots in this paper we use degrees, while we use radiant in our theoretical discussions and in the computer programs. Fig. 1 is obtained by sorting all n_{dat} values of v_{10} in our time series in ascending order and increasing the values of F_{10} by $1/n_{\text{dat}}$ whenever a measured value of v_{10} is encountered. Using a heapsort approach, the sorting is done in $n_{\text{dat}} \log_2(n_{\text{dat}})$ steps (see, e.g., Ref. [7]).

Next we divide the ordinate between 0 and 1 into n_{tab} equal segments. The value of n_{tab} has to be small enough that a table of size $n \times n_{\text{tab}}$ fits conveniently into the computer RAM. For each integer $j = 1, \dots, n_{\text{tab}}$ the value $F_{i,j} = j/n_{\text{tab}}$ defines a unique value $v_{i,j}$ through $F_{i,j} = F_i(v_{i,j})$ as is indicated in the figure (for which $i = 10$). Further, for each choice of a dihedral angle (i.e., a particular value of i) we define the differences

$$\Delta v_{i,j} = v_{i,j} - v_{i,j-1} \quad \text{with} \quad v_{i,0} = -\pi . \quad (6)$$

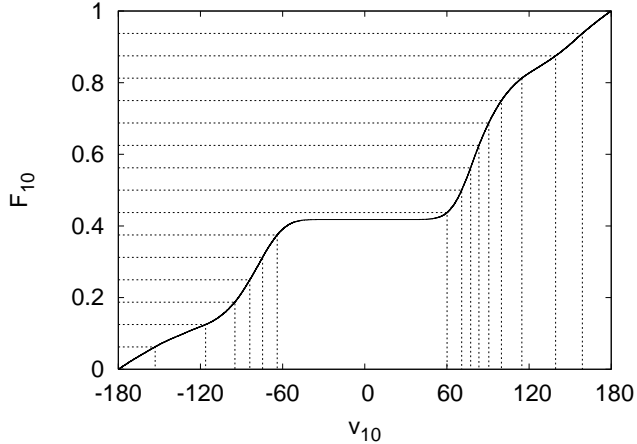


FIG. 1. Estimate of the cumulative distribution function for the Met-Enkephalin dihedral angle v_{10} (Gly-3 ϕ) at 400 K.

The grid in Fig. 1 shows the discretization for the variable v_{10} and the choice $n_{\text{tab}} = 16$. While the discretization for F_{10} on the ordinate is uniformly spaced, widely varying intervals are obtained for v_{10} on the abscissa. The Metropolis procedure for one update of a dihedral angle v_i is now defined as follows:

1. Place the present angle v_i on the discretization grid, i.e., find the integer j through the relation $v_{i,j-1} \leq v_i < v_{i,j}$.
2. Pick an integer j' uniformly distributed in the range 1 to n_{tab} .
3. Propose $v'_i = v_{i,j'-1} + x^r \Delta v_{i,j'}$, where $0 \leq x^r < 1$ is a uniformly distributed random number.
4. Accept v'_i with the probability

$$p_a = \min \left[1, \frac{\exp(-\beta E') \Delta v_{i,j'}}{\exp(-\beta E) \Delta v_{i,j}} \right]. \quad (7)$$

It is through the widely varying ratios $\Delta v_{i,j'}/\Delta v_{i,j}$ that importance sampling for the rugged variables becomes improved. Back to our illustration in Fig. 1: The short and the long interval on the abscissa are proposed with equal probabilities, i.e., the a-priori probability for our angle is high in short intervals and low in long intervals. The CPU time consumption of the RM₁ scheme is practically identical with that of the conventional Metropolis algorithms, because the bulk of the CPU time is spent on the calculation of the new energy E' .

A. Numerical results

Our Metropolis simulations are performed with a variant of SMMP [9] (Simple Molecular Mechanics for Pro-

teins). For each simulation a time series of $2^{17} = 131,072$ configurations is kept, in which subsequent configurations are separated by 32 sweeps. A sweep is defined by updating each dihedral angle once, which we do in the sequential order of the angles listed in table I. Usually sequential updating is more efficient than random updating [7]. Before starting with the measurements, $2^{18} = 262,144$ sweeps are performed for reaching equilibrium. Thus, the entire simulation at one temperature relies on $2^{18} + 32 \cdot 2^{17} = 4,456,448$ sweeps. On a 1.9 GHz Athlon PC this takes under 12 hours. For each dihedral angle the acceptance rate of the Metropolis algorithm was monitored at run time and, following the recipes of [7], the integrated autocorrelation time τ_{int} is calculated from the recorded time series.

Acceptance rates for dihedral angle movements are compiled in table I. For the energy it is the average over all proposed moves. Results are given for simulations with the conventional Metropolis algorithm at 400 K and 300 K, and for the RM₁ simulations at 300 K. The RM₁ updating relies on a discretization with $n_{\text{tab}} = 2^7 = 128$ from the 400 K Metropolis data. Acceptance rates greater than 0.3 are desirable, see [7]. From the table we notice that the acceptance rate varies greatly from angle to angle. For the Metropolis simulation the values at 400 K are in the interval $[0.041, 0.497]$ and at 300 K in $[0.025, 0.387]$. For both temperatures v_9 corresponds to the lowest value, while v_3 and v_{21} correspond to the highest values.

Our RM₁ updating at 300 K increases the acceptance rate for each angle, often even beyond the Metropolis acceptance rate at 400 K, as is obvious from the average value listed for the energy. A second look reveals that the increase in the acceptance rate varies greatly from angle to angle. While for some angles the problem of low acceptance rates is entirely solved, for others the improvement remains modest. For instance for all ω angles the increase is dramatic, e.g., from 0.034 to 0.416 for v_6 . Angles with little improvements are v_7 (0.045 \rightarrow 0.076), v_8 (0.038 \rightarrow 0.064), v_{10} (0.035 \rightarrow 0.070), and v_{11} (0.040 \rightarrow 0.077). Better, but still not particularly impressive, is the increase in the acceptance rates of v_5 , v_{15} and v_{16} . All these are ϕ , ψ angles around C_α atoms. For all other angles RM₁ updating has moved the acceptance rate above or at least close to 0.3.

This situation of ω angles is most easily understood. Figure 2 shows the cumulative distribution function for v_9 (Gly-2 ω) at 400 K, which is the angle of lowest acceptance rate in the conventional Metropolis updating. This distribution function corresponds to a histogram narrowly peaked around $\pm\pi$, which is explained by the specific electronic hybridization of the CO-N peptide bond. From the grid shown in Fig. 2 it is seen that the RM₁ updating concentrates the proposal for this angle in the range slightly above $-\pi$ and slightly below $+\pi$. So the procedure has a similar effect as the often used restriction to the range $[\pi - \pi/9, \pi + \pi/9]$, which is also the default implementation in SMMP (the range $[\pi, \pi + \pi/9]$

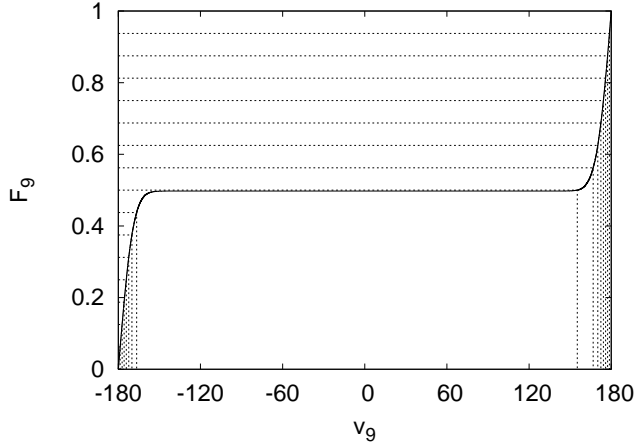


FIG. 2. Estimate of the cumulative distribution function for the Met-Enkephalin dihedral angle v_9 (Gly-2 ω) at 400 K.

is, of course, $[-\pi, -\pi + \pi/9]$ in our plots).

Although acceptance rates give some insights, the decisive quantity for the performance of an algorithm is the more difficult to calculate integrated autocorrelation time τ_{int} . To achieve a pre-defined accuracy, the computer time needed is directly proportional to τ_{int} .

In table II the integrated autocorrelation times are compiled for all angles and for the energy. The values are statistically consistent with those of Ref. [1]. Deviations are due to re-runs and using different procedures for estimating integrated autocorrelation times. They are given in units of 32 sweeps, as this was the step-size of our MC time series. Error bars are shown in parenthesis. For these calculations we used the routines of Ref. [7] together with a jackknife error analysis as explained there. The angles $v_7, v_8, v_{10}, v_{11}, v_{15}$ and v_{16} exhibit very large autocorrelations. Note that four of these are those with the worst improvement of acceptance rates when moving to the RM₁ updating, while two others belong to the subsequent group with still rather poor improvement.

Most remarkable for the angles $v_7, v_8, v_{10}, v_{11}, v_{15}$ and v_{16} is the strong increase of their integrated autocorrelation times when the temperature of the conventional Metropolis simulation is lowered from 400 K to 300 K. For instance, τ_{int} increases for v_7 (Gly-2 ϕ) by almost a factor of twenty, from 5.8 to 103. This reflects that the standard Metropolis algorithm is efficient at 400 K but not so at 300 K. On the other hand the distribution of the variables is not dramatically changed, at least to the extent that this can be judged from one-variable histograms, as is illustrated in Ref. [1] for v_{10} . This is the reason why the 400 K simulation provides useful input for the RM₁ simulation at 300 K.

The RM₁ updating reduces the integrated autocorrelation times at 300 K by factors of about two, for instance for v_7 from 103 to 53. The τ_{int} values vary greatly

TABLE II. Integrated autocorrelation times for dihedral angle movements. Results from simulations in vacuum.

var	400 K	300 K	300 K	300 K
	Metro	Metro	RM ₁	RM ₂
v_1	2.11 (06)	15.2 (1.5)	9.07 (58)	6.03 (47)
v_2	1.18 (02)	2.70 (16)	1.63 (09)	1.70 (12)
v_3	1.03 (01)	2.18 (14)	1.26 (04)	1.24 (04)
v_4	1.44 (03)	4.44 (23)	3.28 (21)	2.82 (14)
v_5	5.44 (20)	54.5 (5.4)	26.3 (1.5)	20.0 (1.3)
v_6	2.95 (07)	23.3 (2.7)	8.65 (58)	6.00 (34)
v_7	5.83 (29)	103 (14)	52.9 (4.3)	24.3 (1.3)
v_8	7.36 (22)	125 (12)	74.2 (6.9)	35.0 (2.7)
v_9	4.39 (13)	32.0 (2.2)	14.2 (1.0)	8.84 (48)
v_{10}	9.08 (88)	124 (12)	80.6 (6.9)	34.3 (2.8)
v_{11}	5.39 (45)	105 (08)	72.4 (5.5)	31.3 (1.9)
v_{12}	3.37 (08)	15.6 (1.5)	5.68 (39)	3.92 (17)
v_{13}	1.81 (05)	8.79 (46)	5.69 (54)	3.59 (22)
v_{14}	1.15 (02)	1.65 (10)	1.40 (07)	1.26 (06)
v_{15}	6.72 (28)	105 (12)	45.6 (2.7)	27.5 (4.5)
v_{16}	9.28 (28)	133 (09)	75.2 (5.2)	33.9 (2.1)
v_{17}	1.90 (04)	9.69 (79)	3.89 (36)	2.29 (08)
v_{18}	1.66 (05)	12.0 (1.6)	6.48 (78)	5.11 (28)
v_{19}	1.17 (02)	1.65 (08)	1.16 (03)	1.17 (03)
v_{20}	1.02 (01)	1.08 (02)	1.03 (02)	1.02 (02)
v_{21}	1.00 (01)	1.00 (01)	1.00 (01)	1.02 (01)
v_{22}	3.20 (12)	35.9 (4.0)	18.2 (1.2)	12.0 (0.8)
v_{23}	1.50 (04)	20.3 (1.8)	11.0 (0.6)	5.96 (35)
v_{24}	1.07 (02)	1.22 (05)	1.00 (01)	1.00 (01)
E	4.89 (21)	50.7 (5.0)	26.0 (1.4)	14.2 (0.7)

from angle to angle. While some angles show no autocorrelations after 32 sweeps ($\tau_{\text{int}} = 1$ or close to it), the largest value on record for RM₁ updating at 300 K is $\tau_{\text{int}} = 80 \pm 7$ for v_{10} (down from 124 for Metropolis updating at 300 K). That the RM₁ updating does not reduce the large autocorrelation times more efficiently has obviously to do with correlations between different angles. Notably even moves of some of the ω angles, like v_9 with $\tau_{\text{int}} = 14.2 \pm 1.0$ appear considerably correlated with the rest of the molecule. RM variants which move several dynamical variables collectively are required and our RM₂ implementation for simultaneous updates of two dihedral angles is discussed in section II. First we address a multi-hit Metropolis procedure.

B. Multi-hit updating

Our sequential updating hits each angle once. The greatly varying integrated autocorrelation times of table II suggest that the computer time may be more efficiently used by performing several Metropolis hits for variables with large integrated autocorrelation times, to be called “bad” variables in the following.

To find a good choice for the number of hits per vari-

able requires some thought. At 300 K the integrated autocorrelation times of the dihedral angles vary between $\tau_{\text{int}} = 1$ and $\tau_{\text{int}} \approx 133$ for the conventional Metropolis updating and still between $\tau_{\text{int}} = 1$ and $\tau_{\text{int}} \approx 80$ for the RM₁ algorithm. It is certainly not a good idea to choose the number of hits per variable in proportion to τ_{int} , because we expect correlations between angles to be the main obstacle for reducing large integrated autocorrelation times. A scheme with a large number of hits mimics the heat-bath algorithm (e.g., Ref. [7]), which does not address correlations between angles. So, a modest increase of the number of hits per bad variable may increase the performance of the updating, while a further increase would result in the contrary.

TABLE III. Multi-hit Metropolis performance.

var	48	400 K	300 K	39	300 K	300 K
	hits	Metro	Metro	hits	RM ₁	RM ₂
v_1	2	2.05 (07)	14.2 (1.1)	1	7.29 (52)	4.47 (21)
v_2	1	1.37 (03)	3.29 (23)	1	1.56 (04)	1.69 (04)
v_3	1	1.04 (04)	2.15 (10)	1	1.39 (04)	1.37 (03)
v_4	1	1.47 (03)	5.49 (57)	1	2.74 (12)	2.52 (12)
v_5	3	3.73 (08)	48.1 (5.7)	2	21.8 (1.7)	15.5 (0.8)
v_6	1	4.19 (09)	19.3 (1.2)	1	7.12 (35)	5.23 (35)
v_7	4	3.96 (21)	61.7 (3.5)	4	42.3 (2.9)	16.1 (0.7)
v_8	4	5.06 (19)	81.8 (5.2)	4	50.5 (4.1)	22.8 (1.5)
v_9	2	4.21 (13)	25.0 (1.6)	1	12.7 (1.0)	6.79 (38)
v_{10}	4	5.28 (20)	86.1 (6.4)	4	48.0 (4.4)	21.3 (1.6)
v_{11}	4	3.72 (14)	81.1 (7.2)	4	53.7 (4.8)	20.3 (1.0)
v_{12}	2	3.04 (13)	11.3 (0.6)	1	4.82 (42)	3.63 (20)
v_{13}	1	2.39 (05)	9.36 (96)	1	4.36 (29)	3.15 (13)
v_{14}	1	1.34 (03)	2.03 (15)	1	1.23 (03)	1.25 (03)
v_{15}	4	4.65 (16)	61.1 (4.4)	2	35.5 (3.2)	17.4 (1.2)
v_{16}	4	6.29 (20)	86.7 (8.5)	2	61.5 (5.0)	24.7 (0.8)
v_{17}	1	2.86 (06)	7.48 (42)	1	3.16 (30)	2.19 (08)
v_{18}	1	2.03 (05)	11.7 (1.1)	1	7.79 (91)	5.57 (35)
v_{19}	1	1.64 (04)	2.57 (15)	1	1.16 (02)	1.26 (02)
v_{20}	1	1.09 (01)	1.21 (02)	1	1.01 (01)	1.02 (01)
v_{21}	1	1.00 (01)	1.02 (02)	1	1.00 (01)	1.00 (01)
v_{22}	2	2.98 (08)	26.2 (1.8)	1	19.2 (1.6)	10.9 (0.7)
v_{23}	1	1.51 (05)	13.3 (1.1)	1	11.4 (1.0)	4.81 (28)
v_{24}	1	1.44 (03)	1.63 (04)	1	1.02 (01)	1.03 (02)
E		4.25 (17)	32.9 (1.4)		24.9 (2.2)	11.0 (0.5)

A guideline for choosing the number of hits is obtained from the observation that the previously obtained acceptance rates per update attempt do not change when performing multiple hits. It appears reasonable to increase the hits of bad variables while bounding the number of hits times the acceptance rate by 0.3 from above. As the acceptance rates change considerably when switching from regular Metropolis to RM₁ updating, we employ different schemes for the two cases. Results for the two different multi-hit schemes are collected in table III.

The numbers in the first “hits” column are used together with the regular Metropolis updating. They are

arranged to add up to 48, i.e., twice the total number of variables. The additional computer time needed is balanced by reducing the number of sweeps between measurements from 32 to 16 (a sweep is now defined by applying the new updating procedure in sequential order once to each angle). By comparing tables II and III we see that the multi-hit updating improves the Metropolis algorithm at 300 K considerably, the integrated autocorrelation time for the energy is down by about 40%.

The numbers in the second “hits” column are used together with RM₁ and RM₂ updating. As RM₁ updating increases acceptance rates already significantly, there is little opportunity for additional improvements due to multiple hits. By that reason the numbers of the column add only up to 39 hits per sweep. This is balanced by reducing the number of sweeps between measurements from 32 to 20 (the integer nearest to $32 \times 24/39$). Using as indicator the integrated autocorrelation time of the energy, the overall improvement found is only a modest 5% when comparing to RM₁ without multiple hits. However, this number increases again to 20% for RM₂ updating (see the subsequent section), as it is then advantageous to spend additional CPU time on the simultaneous moves of two angles.

II. THE RM₂ APPROXIMATION

For the RM₂ approximation we have to generalize the RM₁ scheme of Eq. (7) to the simultaneous updating of two dihedral angles. For $i_1 \neq i_2$ the reduced two-variable pds are defined by

$$\rho_{i_1, i_2}^2(v_{i_1}, v_{i_2}; T) = \int_{-\pi}^{+\pi} \prod_{j \neq i_1, i_2} dv_j \rho(v_j, \dots, v_n; T) . \quad (8)$$

With the one-variable cumulative distribution functions F_{i_1} and a discretization $v_{i_1, j}$, $j = 0, \dots, n_{\text{tab}}$ already given by Eqs. (5) and (6), we define conditional cumulative distribution functions by

$$F_{i_1, i_2, j}(v) = \int_{-\pi}^v dv_{i_2} \int_{v_{i_1, j-1}}^{v_{i_1, j}} dv_{i_1} \rho_{i_1, i_2}^2(v_{i_1}, v_{i_2}) \quad (9)$$

for which the normalization $F_{i_1, i_2, j}(\pi) = 1/n_{\text{tab}}$ holds. To extend the RM₁ updating to two variables we define for each integer $k = 1, \dots, n_{\text{tab}}$ the value $F_{i_1, i_2, j, k} = k/(n_{\text{tab}})^2$. Next we define $v_{i_1, i_2, j, k}$ through $F_{i_1, i_2, j, k} = F_{i_1, i_2, j}(v_{i_1, i_2, j, k})$ and also the differences

$$\Delta v_{i_1, i_2, j, k} = v_{i_1, i_2, j, k} - v_{i_1, i_2, j, k-1} \quad \text{with} \quad v_{i_1, i_2, j, 0} = -\pi . \quad (10)$$

The RM₂ Metropolis procedure for the simultaneous update of (v_{i_1}, v_{i_2}) is then defined as follows:

1. Find the grid index j for the present angle v_{i_1} through $v_{i_1, j-1} \leq v_{i_1} \leq v_{i_1, j}$ as for RM₁ updating.

2. Find the grid index k for the present angle v_{i_2} through $v_{i_1, i_2; j, k-1} \leq v_{i_2} \leq v_{i_1, i_2; j, k}$.
3. Pick two integers j' and k' , each uniformly distributed in the range 1 to n_{tab} . (This could be extended to cover asymmetric ranges $n_{\text{tab}}^1 \times n_{\text{tab}}^2$.)
4. Propose $v'_{i_1} = v_{i_1, j'-1} + x_1^r \Delta v_{i_1, j'}$, where $0 \leq x_1^r < 1$ is a uniformly distributed random number.
5. Propose $v'_{i_2} = v_{i_1, i_2; j', k'-1} + x_2^r \Delta v_{i_1, i_2; j', k'}$, where $0 \leq x_2^r < 1$ is a second uniformly distributed random number.
6. Accept (v'_{i_1}, v'_{i_2}) with the probability

$$p_a^2 = \min \left[1, \frac{\exp(-\beta E') \Delta v_{i_1, j'} \Delta v_{i_1, i_2; j', k'}}{\exp(-\beta E) \Delta v_{i_1, j} \Delta v_{i_1, i_2; j, k}} \right]. \quad (11)$$

The bookkeeping for this process is a bit tricky, because an accepted update changes not only $(j, k) \rightarrow (j', k')$, but also the j from the RM_1 updating of the angles. The latter corresponds to a different table and needs to be re-calculated from the new value of the angle, which can be done in $\log_2(n_{\text{tab}}/2)$ steps. Similarly accepted RM_1 updates can change the initial RM_2 (j, k) values, so that they may have to be re-calculated. We have checked the correctness of our updating procedure by comparing high precision energy averages and other observables with results from previous calculations.

As before, estimates of the conditional cumulative distribution functions, and then of the intervals $\Delta v_{i_1, i_2; j, k}$, are obtained from the conventional Metropolis simulation at 400 K. In the following we focus on the pairs (v_7, v_8) , (v_{10}, v_{11}) and (v_{15}, v_{16}) . These angles correspond to the largest integrated autocorrelation times of the RM_1 procedure and are expected to be strongly correlated with one another because they are pairs of dihedral angles around a C_α atom.

The bias of the acceptance probability given in Eq. (11) is governed by the areas

$$\Delta A_{i_1, i_2; j, k} = \Delta v_{i_1, j} \Delta v_{i_1, i_2; j, k}.$$

For $i_1 = 6$ and $i_2 = 7$ our 400 K estimates of these areas are depicted in Fig. 3. For the RM_2 procedure these areas take the role which the intervals on the abscissa of Fig. 1 play for RM_1 updating. The small and the large areas are proposed with equal probabilities, so the a-priori probability for our two angles is high in a small and low in a large area. In Fig. 3 the largest area is 503.4 times the smallest area. Areas of high probability correspond to allowed regions in the Ramachandran map of a Gly residue [14].

Note that the order of the angles matters. The difference between Fig. 3 and Fig. 4 is that we plot in Fig. 3 the areas $A_{7,8;j,k}$ and in Fig. 4 the areas $A_{8,7;j,k}$ while

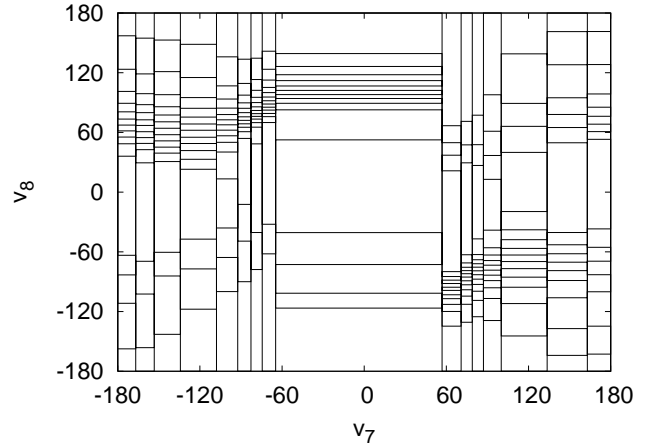


FIG. 3. Areas of equal probabilities (sorting v_7 then v_8).

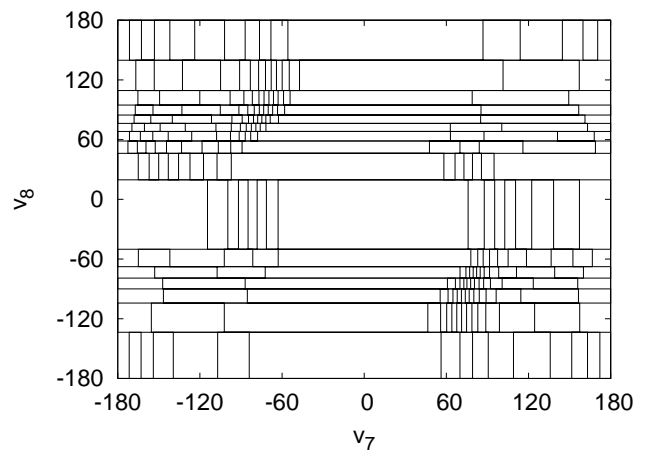


FIG. 4. Areas of equal probabilities (sorting v_8 then v_7).

the labeling of the axes is identical. This means that for Fig. 3 sorting is first done on the angle v_7 (regardless of the value of v_8) and then first done on v_8 for which the corresponding value of v_7 is within a particular bin Δv_7 , but for Fig. 4 it is first done on v_8 and then on v_7 . In Fig. 4 the largest area is 396.4 times the smallest area.

Fig. 5 and Fig. 6 give plots for the (v_{10}, v_{11}) and (v_{15}, v_{16}) pairs in which the angle with the smaller subscript is sorted first. The ratio of the largest area over the smallest area is 650.9 for (v_{10}, v_{11}) and 2565.8 for (v_{15}, v_{16}) . The large number in the latter case is related to the fact that (v_{15}, v_{16}) is the pair of ϕ, ψ angles around the C_α atom of Phe-4, for which positive ϕ values are disallowed [14].

The RM_2 scheme which we have tested adds updates for the three pairs (v_7, v_8) , (v_{10}, v_{11}) and (v_{15}, v_{16}) to our RM_1 moves. In each case both orders of sorting are used, so that we add altogether six new updates. Six RM_2 update tables of size 16×16 are built from the 400 K

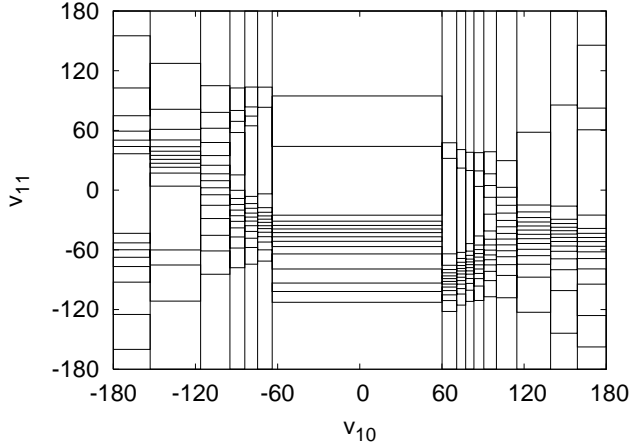


FIG. 5. Areas of equal probabilities (sorting v_{10} then v_{11}).

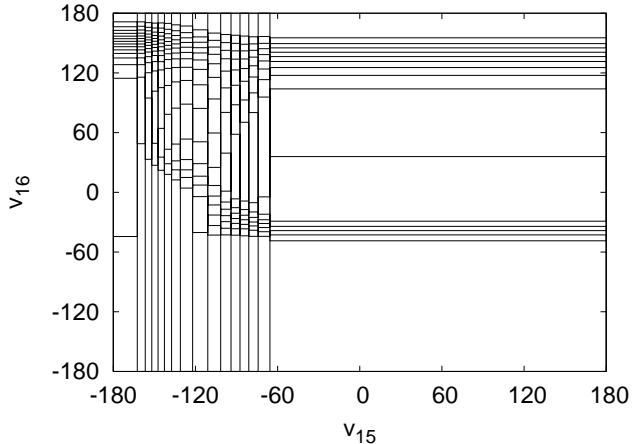


FIG. 6. Areas of equal probabilities (sorting v_{15} then v_{16}).

Metropolis simulation and the areas of four of them are precisely those shown in Figs. 3 to 6. The acceptance rates of the one-variable updates remain the same as they were for RM_1 procedure. For the acceptance rate of a pair we average over the two cases. Table IV compares the two-angle RM_2 acceptance rates at 300 K to those obtained by proposing the same two-angle updates with the standard Metropolis procedure. At 300 K an increase by factors in the range from three to nearly ten is found. However, the values remain surprisingly low, presumably due to substantial correlations with additional angles.

Integrated autocorrelation times are calculated to evaluate the improvement of the overall performance. For this purpose the number of sweeps between measurements is reduced from 32 to 26 to account for the additional CPU time needed for the two-angle moves. The results are presented in table II. Despite the small acceptance rates for the two-angle moves, the integrated

TABLE IV. Acceptance rates for simultaneous moves of angle pairs.

variable pair	400 K	300 K	300 K	300 K
	Metro	Metro	RM_2	RM_2
			$n_{\text{tab}} = 16$	$n_{\text{tab}} = 128$
(v_7, v_8)	0.044	0.0060	0.019	0.020
(v_{10}, v_{11})	0.041	0.0051	0.021	0.022
(v_{15}, v_{16})	0.018	0.0051	0.048	0.050

autocorrelation times for the targeted angles are substantially reduced. For all six angles they are smaller by factors larger than two when compared with the RM_1 results. Interestingly this speed-up propagates through the entire system and the integrated autocorrelation time for the energy is found to be about a factor of two smaller than for the RM_1 algorithm.

Despite their relatively low acceptance rates the two-angle moves lead to substantial improvements. Multi-hit updates allow us to focus even more on these moves. For the one-angle updates we use the same numbers of hits as for RM_1 updating (see table III). In addition we use four hits for the pairs (v_7, v_8) and (v_{10}, v_{11}) , and two hits for the (v_{15}, v_{16}) pair. As in each case both orders of the updating are used, this amounts to a multiplication of the acceptance rates of table IV by eight for the first two pairs and by four for the last pair (i.e., we stay well below our 0.3 bound). Altogether we perform then 39 one-angle and 20 two-angle hits per sweep, which is balanced by reducing the number of sweeps between measurements to 13 (the integer nearest to $32 \times 24/59$). The integrated autocorrelation time for the energy decreases then by about 20% from 14 (table II) to 11 (table III). Obviously, it is important to focus on multi-angle updates.

III. SUMMARY AND CONCLUSIONS

We have reviewed the one-variable approximation RM_1 of the rugged Metropolis (RM) scheme of Ref. [1] and worked out a two-variable approximation RM_2 for simultaneous moves of two dihedral angles. As before the testing ground has been Met-Enkephalin and a gain of a factor of four over conventional Metropolis simulations was demonstrated at 300 K. In comparison the gain in real time at 300 K due to using the replica exchange method between the temperatures 400 K and 300 K was a factor of about 2.5 [1] (at the cost of using two processors, while getting simultaneously results at both temperatures).

Although the elaboration of the RM scheme is seen to be on track, much work is left to be done. Even for a system as simple as Met-Enkephalin it remains unclear which kinds of correlations are responsible for the still low acceptance rates of the two-angles moves. On the other hand it is encouraging to see that the autocorrelations times of these angles are nevertheless substantially

reduced and that this effect propagates through the entire system. Other test cases need to be investigated to get a broader understanding of the observed features. In particular one would like to know how the performance gain depends on the system size.

Presently the leading method for simulations of biomolecules is molecular dynamics (see [15] for a textbook). This is to some extent surprising, because Markov Chain Monte Carlo (MC) simulations allow for large changes of conformations in a single move, so thermodynamically relevant equilibrium configurations can, in principle, be reached quickly. However, in simulations of biomolecules with an explicit inclusion of solvent interactions, large MC moves face the problem that there will not be a suitable cavity in the solvent to accommodate a large distortion of the molecule shape. While the RM method discussed in this paper decreases the likelihood of steric clashes in a vacuum simulation, it has no immediate translation into the situation of explicit solvent models.

The way out may be the use of implicit solvent models, for which the change in the molecule-solvent and solvent-solvent interaction energies can be calculated instantaneously, like in a vacuum simulation. Indeed RM₁ simulations for implicit solvent models, based on the solvent-accessible area method implemented in [9], have already been performed [16]. The algorithmic improvements were similar as found for the vacuum situation. However there is evidence [17,16] that the class of solvent models used does not parametrize the solvent interactions properly.

It appears that quite generally the reliability of implicit solvent models has not yet been well established. Numerically this can possibly be overcome by an iterative approach. With our algorithms we can reliably generate a large number of equilibrated and statistically independent configurations in vacuum. It is reasonable to assume that the relaxation time scale of the solvent about a biomolecule of fixed shape is short. So we can calculate the solvent-solvent and solvent-molecule mean energies for a large number of static conformations by equilibrating the surrounding solvent explicitly. The parameters for an implicit solvent model can then be obtained by least square fits to these mean energies. The resulting parameterization defines a first approximation to an implicit solvent model. We can then generate a large number of statistically independent configurations in this approximation and iterate this process until satisfactory agreement between the implicit model and the explicit solvent energy calculations is obtained, or it becomes obvious that the chosen implicit parameterization will not lead to convergence.

Finally we like to mention that MC moves may be fine-tuned on a local level as done in the approach of Ref. [18]. This is also possible for models which include solvents explicitly. So MC may still be a viable alternative to molecular dynamics for explicit solvent models.

ACKNOWLEDGMENTS

Our calculations were performed on the Anfinen PC cluster of FSU's School of Computational Science. H.-X. Zhou was supported in part by the National Institutes of Health grant GM 58187.

-
- [1] B.A. Berg, Phys. Rev. Lett **90**, 180601 (2003).
 - [2] D. Bryngelson and P.G. Wolynes, Proc. Nat. Acad. Sci. USA **84**, 7524 (1987).
 - [3] G. La Penna, S. Morante, A. Perico, and G.C. Rossi, J. Chem. Phys. **121**, 10725 (2004); B. Berg, H. Noguchi, and Y. Okamoto, Phys. Rev. E **68**, 036126 (2003); U.H.E. Hansmann, Physica A **321**, 152 (2003); A. Mitsutake, Y. Sugita and Y. Okamoto, Biopolymers (Peptide Science) **60**, 96 (2001).
 - [4] N. Go and H.A. Scheraga, Macromolecules **3**, 178 (1970).
 - [5] J.P. Ulmschneider and W.L. Jorgensen, J. Chem. Phys. **118**, 4261 (2003).
 - [6] Z. Li and H.A. Scheraga, Proc. Nat. Acad. Sci. USA, **85**, 6611 (1987).
 - [7] B.A. Berg, *Markov Chain Monte Carlo Simulations and Their Statistical Analysis*, World Scientific, 2004.
 - [8] M.J. Sippl, G. Nemethy, and H.A. Scheraga, J. Phys. Chem. **88**, 6231 (1984) and references given therein.
 - [9] F. Eisenmenger, U.H. Hansmann, S. Hayryan, and C.-K. Hu, Comp. Phys. Commun. **138**, 192 (2001).
 - [10] A.D. Bruce, J. Phys. A **18**, L873 (1985).
 - [11] Milchev, D.W. Heermann, and K. Binder, J. Stat. Phys. **44**, 749 (1986).
 - [12] M.W. Deem and J.S. Bader, Mol. Phys. **87**, 1245 (1996).
 - [13] G. Favrin, A. Irback, and F. Sjunnesson, J. Chem. Phys. **114**, 8154 (2001).
 - [14] G.E. Schultz and R.H. Schirmer, *Principle of Protein Structure*, Springer, New York, 1979.
 - [15] D. Frenkel and B. Smit, *Understanding Molecular Simulation*, Academic Press, San Diego, 1996.
 - [16] B.A. Berg and H.-P. Hsu, Phys. Rev. E **69**, 026703 (2004).
 - [17] Y. Peng, U.H. Hansmann, and N.A. Alves, J. Chem. Phys. **118**, 2374 (2003); Y. Peng and U.H. Hansmann, Biophys. J. **82**, 3269 (2003).
 - [18] D. Bouzida, S. Kumar, and R. Swendsen, Phys. Rev. A, **45**, 8894 (1992).